JOURNAL OF SOLID STATE CHEMISTRY **123,** 83–92 (1996)
ARTICLE NO. 0155

Keggin Cluster Formation by Hydrothermal Reaction of Tungsten Trioxide with Methyl Substituted Ammonium: The Crystal Structure of Two Novel Compounds, $[NH_2(CH_3)_2]_6H_2W_{12}O_{40} \cdot {\sim}4H_2O$ and $[N(CH_3)_4]_6H_2W_{12}O_{40} \cdot 2H_2O$

Peter Zavalij,* Jingdong Guo,* M. Stanley Whittingham,* Robert A. Jacobson,† Vitalij Pecharsky,†
Cordelia K. Bucher,‡ and Shiou-Jyh Hwu§

**Department of Chemistry and Materials Research Center, State University of New York at Binghamton, Binghamton, New York 13902-6000; †244 Spedding Hall, Ames Laboratory, Iowa State University, Ames, Iowa 50011-3020; ‡Department of Chemistry, Rice University, P.O. Box 1892, Houston, Texas 77251; and §Department of Chemistry, Clemson University, Clemson, South Carolina 29634*

Received September 5, 1995; in revised form January 23, 1996; accepted January 25, 1996

Tungsten(VI) oxides can be formed by mild hydrothermal reactions, with the exact crystalline structure being determined by the cations in solution. The impact on the reaction between tungstic acid and ammonium ions as the hydrogen atoms are systematically substituted by methyl groups is investigated. Ammonium and methylammonium (MA) cations form the pyrochlore structure type $(NH_4)_xWO_{3+x/2} \cdot nH_2O$ (*A*) and $(MA)_xWO_{3+x/2} \cdot nH_2O$ (*B*). Ammonium may also form the hexagonal bronze tunnel structure. Using dimethylammonium (DMA), trimethylammonium (TrMA), and tetramethylammonium (TMA) leads to the formation of well crystallized Keggin structures: $DMA_6[H_2W_{12}O_{40}] \cdot nH_2O$ (*C*), $DMA_6[H_2W_{12}O_{40}] \cdot {\sim}4H_2O$ (*D*), $TrMA_6[H_2W_{12}O_{40}]$ (*E*), $TrMA_6[H_2W_{12}O_{40}] \cdot {\sim}2H_2O$ (*F*), $TMA_6[H_2W_{12}O_{40}] \cdot 2H_2O$ (*G*), and in some cases hexagonal tungsten bronzes. Characterization was done using powder and single crystal X-ray analysis, as well as IR and TGA methods. The pyrochlore structures have been refined by the Rietveld method. The powder patterns were indexed to the orthorhombic system (space group *Pnma*, $a = 21.886(4)$, $b = 21.469(4)$, $c = 13.232(3)$ Å) for *E* and monoclinic system ($P2_1/n$, $a = 19.273(4)$, $b = 12.017(2)$, $c = 12.253(2)$ Å, $\beta = 90.70(1)°$) in the case of *F*. The crystal structures of *D* and *G* were determined by single crystal X-ray analysis. Blue crystals of *D* are orthorhombic, space group *Pnma*, $a = 22.446(3)$, $b = 19.810(3)$, $c = 12.854(2)$ Å, $V_{cell} = 5716$ Å^3, $Z = 4$, $d_{clc} = 3.72$ g/cm^3 (Mo$K\alpha$ radiation, $2\theta_{max.} = 55°$, $R = 0.077$ for 2076 reflections). Dark blue crystals of *G* are orthorhombic, space group *Pnma*, $a = 21.90(1)$, $b = 21.507(7)$, $c = 13.27(1)$ Å, $V_{cell} = 6250$ Å^3, $Z = 4$, $d_{clc} = 3.54$ g/cm^3 (Mo$K\alpha$ radiation, $2\theta_{max.} = 55°$, $R = 0.052$ for 4488 reflections). Both structures consist of a hexagonal close packed arrangement of the almost spherical Keggin anions $[H_2W_{12}O_{40}]^{-6}$. They are not isostructural because of a different orientation of the tungsten clusters.

INTRODUCTION

During investigations of the hydrothermal formation of metastable transition metal oxides that have relatively open structures, we found that the nature of the cations present in solution (the ''templating ion'') has a dramatic effect on the crystal structure of the phase formed, as does the pH, the temperature of the reaction medium, and the selection of transition metals. We previously reported that by using mild hydrothermal methods, such as Na_2WO_4 acidified with HCl and heated in an aqueous environment at 150°C, different crystalline forms of the tungsten(VI) oxides, such as hexagonal tungsten bronze or pyrochlore structures, can be readily synthesized (1, 2). Use of molybdenum(VI) oxide and an inorganic cation yields hexagonal molybdenum oxides (3) with a larger and more flexible one-dimensional channel than tungsten bronzes. More recently, we have carried out this strategy with the larger tetramethylammonium (TMA) templating cation and have synthesized a novel molybdate that has a potentially exciting layered structure (4).

In this paper, we report a systematic investigation of the hydrothermal interaction of tungstic acid with methyl substituted ammonium cations. Reaction of tungstic acid, directed by small ammonium and methylammonium (MA) cations, led to the pyrochlore structure type $(NH_4)_x WO_{3+x/2} \cdot nH_2O$ (*A*) and $(MA)_x WO_{3+x/2} \cdot nH_2O$ (*B*), where *x* is ~1.0. However, under some conditions using the ammonium cation hexagonal bronze structures could be formed. Larger cations such as dimethylammonium (DMA), trimethylammonium (TrMA), and tetramethylammonium under varied experimental conditions led to the formation of five novel compounds that contain the

0022-4596/96 $18.00

TABLE 1
Hydrothermal Synthesis Conditions and Product Description

Ion	Amount	°C	pH 1.5	pH 3.5	pH 5.0
NH_4^+	15 ml conc. aq.	150		greenish powder (*A*)	
MA	10 ml MAOH	150		cream white powder (*B*)	
DMA	10.24 ml 40% aq.	160	amorphous powder, colorless crystals (*C*)	clear solution	—
		210	cyan colored amorphous powder, dark blue flat crystals (*D*)	blue powder, black flat crystals (*D*)	
TrMA	20.26 ml 25% aq.	160	yellow powder (monoclinic WO_3)	dark blue flat crystals (*E*)	—
		210	light blue powder, isometric colorless crystals (*F*)	dark blue crystals (*F*)	black crystals (*F*)
TMA	18 ml 25% aq.	210		dark blue crystals (*G*)	

Keggin type of tungsten cluster: $DMA_6[H_2W_{12}O_{40}] \cdot nH_2O$ (*C*), $DMA_6[H_2W_{12}O_{40}] \cdot \sim 4H_2O$ (*D*), $TrMA_6[H_2W_{12}O_{40}]$ (*E*), $TrMA_6[H_2W_{12}O_{40}] \cdot \sim 2H_2O$ (*F*), and $TMA_6[H_2W_{12}O_{40}] \cdot 2H_2O$ (*G*).

EXPERIMENTAL

Hydrothermal Preparation

Commercial tungstic acid H_2WO_4 (5 g) was mixed with an aqueous solution of substituted ammonium hydroxide. These mixtures were then acidified with 3 *M* HCl to the desired pH, resulting in yellowish gels. These gels were transferred to Teflon-lined Parr acid digestion bombs and heated for 3 days at temperatures of 150, 160, or 210°C under autogeneous pressures. After gradually bringing the temperature down to ambient conditions, the crystals and powders were separately collected, washed with water, and air dried. Very different product types were observed, dependent on temperature and pH. Experimental conditions and product descriptions are listed in Table 1.

TABLE 2
Experimental Crystallographic Data for $(NH_4)_xWO_{3+x/2} \cdot nH_2O$ and $MA_xWO_{3+x/2} \cdot nH_2O$ (Rietveld Refinement)

Parameters		NH_4-pyrochlore	MA-pyrochlore
Space group		*Fd*3*m*	*Fd*3*m*
a (Å)		10.1752 (4)	10.3468 (1)
d_{clc} ($g \cdot cm^{-3}$)		6.0744(7)	5.9452(2)
Used reflections		21	21
R(Bragg), *R*(p)		0.048, 0.091	0.050, 0.085
W	site	16*c* (0, 0, 0)	16*c* (0, 0, 0)
	B(Å^2)	3.21 (5)	2.50 (4)
	G	1	0.95 (2)
O	site	48*f* (*x*, 1/8, 1/8)	48*f* (*x*,1/8, 1/8)
	x	0.3102 (13)	0.3129 (9)
	B(Å^2)	0.0 (4)	2.3 (3)
	G	1	1
NH_4^+ or MA	N site	8*b* (3/8, 3/8, 3/8)	8*b* (3/8, 3/8, 3/8)
	C site		32*e*(*x*, *x*, *x*), $x = 0.443$
	BÅ^2)	3.3 (14)	2.5
	G(N), *G*(C)	1	1, 0.25
W–O distances(Å)		1.900(4) × 6	1.941 × 6

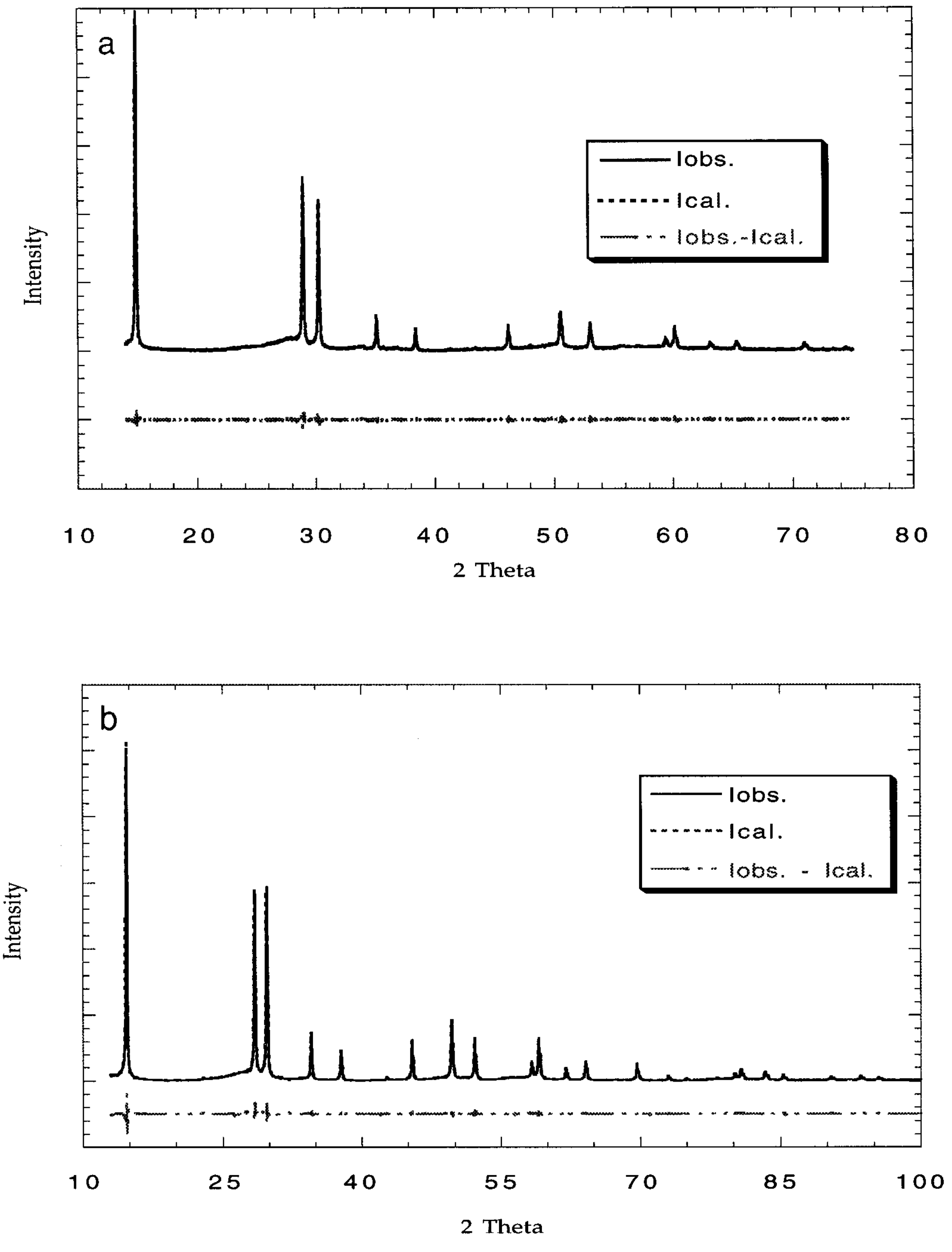

FIG. 1. X-ray diffraction profiles of (a) $(NH_4)_xWO_{3+x/2} \cdot nH_2O$ and (b) $MA_xWO_{3+x/2} \cdot nH_2O$. Solid lines and dots represent observed and calculated intensities, respectively, their difference is plotted on the bottom.

Characterization and Chemical Analysis

The analyses were performed by various techniques. The presence of chlorine was excluded by normal chemical analysis. TGA was done under O_2, and XRD patterns after TGA showed the yellow monoclinic tungsten oxide WO_3. The weight loss was used to find the ratio between tungsten, incorporated ammonium cation, and water. FTIR spectra were collected for all the named compounds, and they showed a terminal oxygen double bonded to the tungsten. In the case of the *C–G* compounds IR spectra showed three strong W–O stretching bands at 930–940, 875–890, and 755–765 cm^{-1} characteristic of keggin-type anions (5).

In the case of the TMA compound, heating the sample to 500°C under continuous purging of He gas, TMA can be driven out and titrated as trimethyl amine with standard HCl. Magnetic susceptibility measurements were done for two batches of compound *F*; colorless ones show purely diamagnetic behavior indicating the oxidation state of

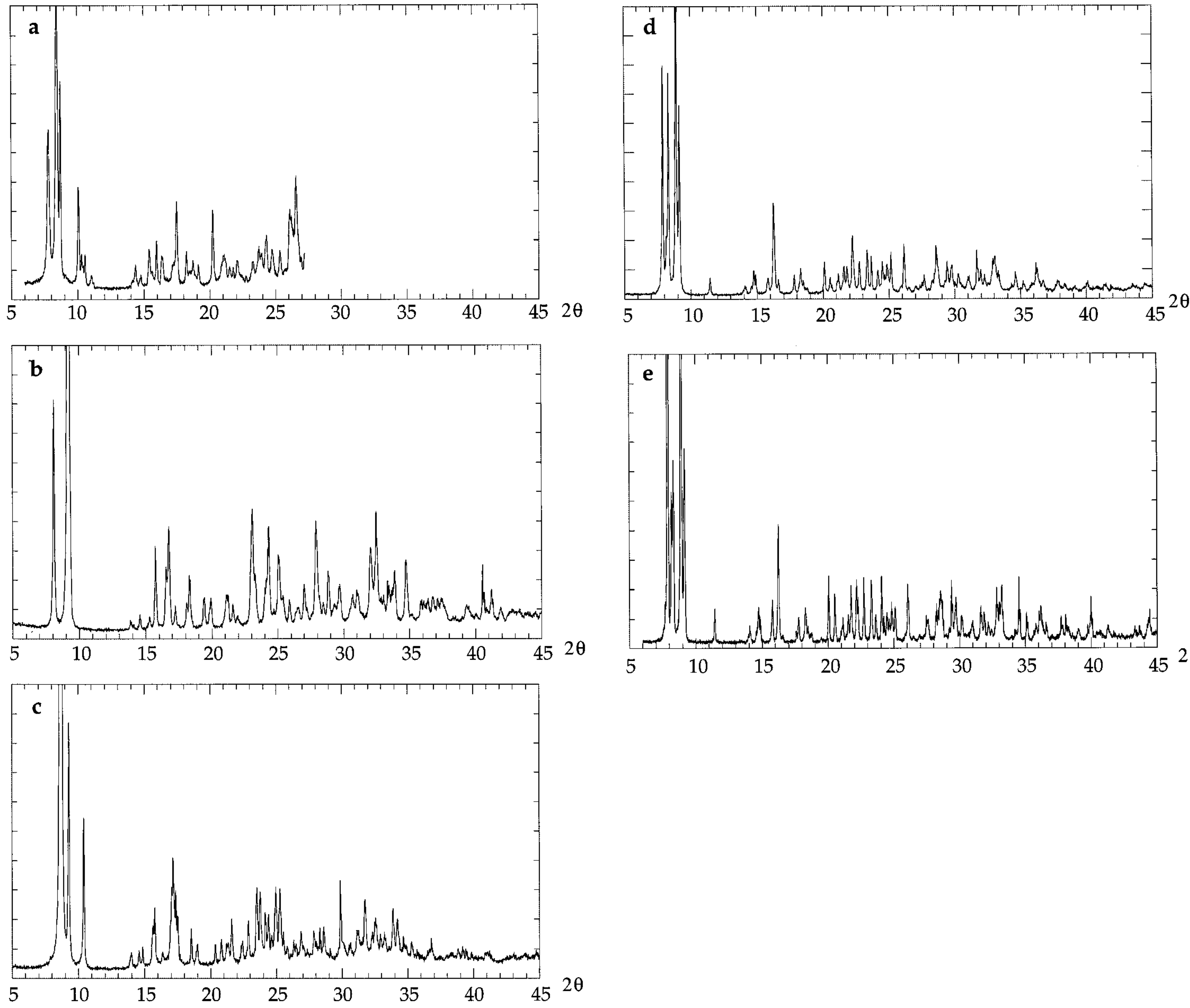

FIG. 2. Powder diffraction profiles for (a) $DMA_6[H_2W_{12}O_{40}] \cdot nH_2O$ (T = 160°C, pH 1.5), (b) $DMA_6[H_2W_{12}O_{40}] \cdot {\sim}4H_2O$ (T = 210°C, pH 3.5), (c) $TrMA_6[H_2W_{12}O_{40}]$ (T = 160°C, pH 3.5), (d) $TrMA_6[H_2W_{12}O_{40}] \cdot {\sim}2H_2O$ (T = 210°C, pH 3.5), (e) $TMA_6[H_2W_{12}O_{40}] \cdot 2H_2O$ (T = 210°C, pH 3.5).

tungsten is VI, and the blue-black sample showed slight paramagnetism (less than 1% of W(V)), probably due to surface reduction or other impurities. Combining all the above information, the compound was best formulated as $[N(CH_3)_4]_6H_2W_{12}O_{40} \cdot 2H_2O$, hexakis-tetramethylammonium α-dihydrododeca-tungstate dihydrate. The crystal structure determination confirmed these analytical results.

CRYSTAL STRUCTURE STUDY

Powder X-Ray Diffraction

X-ray powder diffractometer data (Scintag XDS 2000, Cu$K\alpha$ radiation, Ge solid state detector) was used for identification, purity control, indexing, and unit cell refinement. The crystal structure refinement of *A* and *B* were carried out by using both Bragg's intensities of diffraction peaks and the full profile of the XRD pattern (Rietveld method). Locations of incorporated cations and/or water were found from difference Fourier maps. The final results of Rietveld refinement are listed in Table 2. Figure 1 shows the observed and calculated profile for *A* and *B*. The diffraction patterns of *D–G* compounds (Fig. 2) were successfully indexed. The cell parameters and space groups can be found in Table 3. Computations (indexing and unit cell refinement) were performed by using CSD, a crystallographic programs package (6).

TABLE 3
Composition, Symmetry, and Unit Cells of Novel Keggin Compounds

	Compound	t (°C)	pH	Space group	a (Å)	b (Å) β (°)	c (Å)
A	$(NH_4)_xWO_{3+1/2x} \cdot nH_2O$	150	3.5	$Fd3m$	10.1752(4)		
B	$MA_xWO_{3+1/2x} \cdot nH_2O$	150	3.5	$Fd3m$	10.3468(1)		
C	$DMA_6[H_2W_{12}O_{40}] \cdot {\sim}xH_2O$	160	1.5			unindexed	
D	$DMA_6[H_2W_{12}O_{40}] \cdot {\sim}4H_2O$	210	3.5	$Pnma$	22.411 (5)	19.722(4)	12.711(3)
E	$TrMA_6[H_2W_{12}O_{40}]$	160	3.5	$P2_1/n$	19.273(4)	12.017(2) 90.703(9)	12.253(2)
F	$TrMA_6[H_2W_{12}O_{40}] \cdot {\sim}2H_2O$	210	3.5	$Pnma$	21.886(4)	21.469(4)	13.232(3)
G	$TMA_6[H_2W_{12}O_{40}] \cdot 2H_2O$	200	3.5	$Pnma$	21.899 (4)	21.539 (3)	13.274 (2)

Single Crystal X-Ray Diffraction

$TMA_6[H_2W_{12}O_{40}] \cdot 2H_2O$ (G). The dark blue single crystal of G was investigated at room temperature on an automatic diffractometer CAD-4 (Rice University, Texas) by using graphite-monochromatized Mo$K\alpha$ radiation. Independent reflections (7886) were measured in one octant of reciprocal space to $2\theta_{\text{max.}} = 55°$. All intensities were corrected by counting losses and Lorenz polarization factors. The absorption correction factors were calculated by using empirical ψ-scan data (transmission factors were between 0.48 and 1). The cell parameters ($a = 21.90(1)$, $b = 21.507(7)$, $c = 13.27(1)$ Å) were obtained from least-squares refinement by using 20 reflections in the range 20°–25° 2θ. Systematic absences (Okl: $k + l = 2n$ and $hk0$: $h = 2n$) yielded two possible space groups, the centrosym-

TABLE 4
Experimental Crystallographic Data for $TMA_6[H_2W_{12}O_{40}] \cdot 2H_2O$ and $DMA_6[H_2W_{12}O_{40}] \cdot {\sim}4H_2O$

	Crystal data	
Compound formula	$TMA_6H_2W_{12}O_{40} \cdot 2H_2O$	$DMA_6H_2W_{12}O_{40} \cdot {\sim}4H_2O$
Crystal system	Orthorhombic	Orthorhombic
Space group	$Pnma$	$Pnma$
a	21.90(1) Å	22.446(3) Å
b	21.507(7) Å	19.810(3) Å
c	13.27(1) Å	12.854(2) Å
Cell volume	6250 $Å^3$	5716 $Å^3$
$F(000)$	5932 electrons	5648 electrons
Number of atoms in cell	648	528
Calculated density	3.54 g/cm^3	3.72 g/cm^3
Absorption coefficient	234 cm^{-1}	255 cm^{-1}
	Data collection	
Diffractometer	CAD-4	Siemens P4
Crystal color, Habit	Dark blue, Prism	Blue, Prism
Temperature	23°C	23°C
Radiation, monochromator	Mo$K\alpha$, graphite	Mo$K\alpha$, graphite
2θ and $\sin \theta/\lambda$ (max)	55°, 0.65 $Å^{-1}$	55°, 0.65 $Å^{-1}$
Scan technique and rate	$\theta/2\theta$ 4 °/min	$\theta/2\theta$ 4 °/min
Measured/unique reflect.	7886 7374	5271 5003
Absorption correction	Empirical, ψ scan	Empirical, ψ scan
	Refinement	
Software used	SHELX76, CSD	CSD
Solution	Direct method	Direct method
Least-squares method	Block/full-matrix	Block/full-matrix
Restrictions	$F(hkl) > 6\sigma(F)$	$F(hkl) > 6\sigma(F)$
Weighing scheme	$1/[\sigma(F)^2 + 0.001 \cdot F(\text{obs})^2]$	$1/[\sigma(F)^2 + 0.002 \cdot F(\text{obs})^2]$
Free parameters	388	173
Used reflections	4488	2076
$R(F)$, $R_w(F)$	0.052 0.055	0.077 0.080

metric *Pnma* and noncentrosymmetric $Pn2_1a$. The *Pnma* (No. 62) was preferred after examination of the statistical tests. Later refinement into a noncentrosymmetric group did not give better results. The experimental and refinement conditions are shown in Table 4.

The crystal structure for the title compound was solved and refined by the SHELX76 (7) program. The seven tungsten atoms were found from the best of the direct methods solutions. All oxygen atoms were located by the difference Fourier maps. The next Fourier map, after anisotropic thermal parameters refinement for tungsten and oxygen atoms, contained positions of some nitrogen and carbon atoms of TMA cations. The final refinements were then made using the CSD crystallographic package (6) to an *R* value 0.052. Thermal motions of TMA cations made finding them difficult even on difference maps after anisotropic refinement. It was possible only by using higher angle refinement of the tungsten cluster, which has much lower thermal motions, and lower angle reflections for difference Fourier synthesis. This allowed us to locate all TMA molecules. In some cases, the position of the last (fourth) carbon atom was found by geometrical calculation. The thermal motions of some TMA molecules are so large that one of them split at two different orientations. The resulting atomic coordinates and isotropic (equivalent) temperature parameters are listed in Table 5. Anisotropic thermal motions of the Keggin cluster atoms are shown in Fig. 2a.

$DMA_6[H_2W_{12}O_{40}] \cdot {\sim}4H_2O$ (*D*). The crystals of *D* were investigated at room temperature on a four-circle diffractometer Siemens P4 (Ames Lab, Iowa State University) by using graphite-monochromatized Mo$K\alpha$ radiation. Independent reflections (5271) were measured in one octant of reciprocal space to $2\theta_{\max.} = 55°$. All intensities were corrected by counting losses and Lorenz polarization factors. The absorption correction factors were calculated by using empirical ψ scan data. The cell parameters ($a = 21.446(3)$, $b = 19.810(3)$, $c = 12.854(2)$ Å) were obtained from least-squares refinement by using 23 reflections in the range 20°–26° 2θ.

Despite the fact that the space group and unit cell of *D* and *G* are the same or almost the same, they are not isostructural. In any case, simply taking the *G* model to *D* does not lead to reasonable results. Therefore, the *D* structure was solved by the direct methods in the same way as *G*. The E-map gave the location of tungsten atoms, and the positions of oxygen atoms were found easily enough from difference Fourier syntheses. Unfortunately, we were able to locate just a few DMA cations. Even high angle refinement, described above, did not aid in the location of the remaining DMA cations. This is caused by lower crystal quality as well as higher mobility and thermal motions of the DMA cation. The final refinements were done in anisotropic (only tungsten atoms) and isotropic approximation, which led to $R = 0.077$ (Table 4). The

TABLE 5
Atomic Parameters for $TMA_6[H_2W_{12}O_{40}] \cdot 2H_2O$

Atom	*x*/*a*	*y*/*b*	*z*/*c*	$B_{\text{is/eq}}{}^{a}$ (Å)
W1	0.21975(6)	1/4	0.33745(9)	1.68(3)
W2	0.48217(6)	1/4	0.62870(10)	1.63(3)
W3	0.22273(4)	0.16396(4)	0.57793(7)	1.85(2)
W4	0.34579(4)	0.16453(4)	0.71415(7)	1.70(2)
W5	0.33968(4)	0.17509(4)	0.26076(7)	1.64(2)
W6	0.48079(4)	0.17332(4)	0.41222(7)	1.65(2)
W7	0.34367(4)	0.08943(4)	0.50191(7)	1.83(2)
O1	0.1473(10)	1/4	0.2900(20)	3.0(7)
O2	0.5350(10)	1/4	0.7210(20)	3.1(6)
O3	0.1508(8)	0.1360(8)	0.6045(13)	3.1(5)
O4	0.3578(7)	0.1359(8)	0.8342(12)	2.8(4)
O5	0.3471(8)	0.1234(7)	0.1633(11)	2.8(4)
O6	0.5322(7)	0.1227(7)	0.3657(14)	3.2(5)
O7	0.3527(8)	0.0115(8)	0.4805(11)	3.0(5)
O13	0.2126(6)	0.1895(6)	0.4420(11)	1.9(4)
O15	0.2534(6)	0.1872(7)	0.2487(11)	2.0(4)
O24	0.4271(7)	0.1899(7)	0.6803(11)	2.0(4)
O26	0.5192(6)	0.1863(7)	0.5418(11)	1.8(4)
O33	0.2145(9)	1/4	0.6088(14)	1.6(5)
O34	0.2586(7)	0.1498(6)	0.7080(11)	2.2(4)
O37	0.2575(8)	0.0878(7)	0.5304(11)	2.4(4)
O44	0.3313(10)	1/4	0.7420(16)	2.4(6)
O47	0.3610(7)	0.0864(7)	0.6438(11)	2.3(4)
O55	0.3544(9)	1/4	0.1834(14)	1.6(5)
O56	0.4224(7)	0.1766(7)	0.3063(10)	2.0(4)
O57	0.3254(7)	0.1180(7)	0.3680(11)	2.0(4)
O66	0.5152(8)	1/4	0.3670(15)	1.6(5)
O67	0.4252(7)	0.1168(7)	0.4753(11)	2.2(4)
O155	0.3183(8)	1/4	0.3624(14)	1.3(5)
O266	0.4254(9)	1/4	0.4866(13)	1.3(5)
O347	0.3209(6)	0.1843(6)	0.5578(9)	1.4(3)
O_w	0.413(1)	0.074(1)	0.000(2)	6.6(8)
N1	0.050(1)	0.048(1)	0.782(2)	3.6(6)
C11	0.098(1)	0.094(1)	0.820(3)	4.6(9)
C12	0.080(2)	−0.011(2)	0.743(2)	5.0(9)
C13	0.014(2)	0.083(2)	0.707(3)	5.3(10)
C14	0.012(1)	0.028(1)	0.874(2)	4.2(8)
N2	0.009(2)	1/4	0.474(3)	5.8(14)
C21	0.066(2)	1/4	0.542(4)	6.4(19)
C22	−0.046(2)	1/4	0.538(5)	9.0(25)
C23	0.009(3)	0.308(3)	0.397(4)	16.8(28)
N3	0.201(1)	1/4	0.965(2)	2.6(8)
C31	0.181(2)	1/4	0.862(3)	5.6(16)
C32[b]	0.267	1/4	0.995	8.1
C33[b]	0.175	0.309	1.019	8.1
C32[c]	0.147	1/4	1.041	8.1
C33[c]	0.239	0.193	0.984	8.1
N4	0.193(2)	0.052(2)	0.301(3)	10.0(14)
C41	0.240(2)	0.011(2)	0.259(4)	11.2(18)
C42	0.139	0.015	0.343	22.1
C43	0.166	0.094	0.218	22.1
C44	0.215	0.095	0.384	22.1

[a] $B_{\text{eq}} = 1/3[B_{11}a^{*2}a^2 + B_{22}b^{*2}b^2 + B_{33}c^{*2}c^2 + 2B_{12}a^*b^*ab \cdot \cos\gamma + 2B_{13}a^*c^*ac \cdot \cos\beta + 2B_{23}b^*c^*bc \cdot \cos\alpha]$.

[b] Occupation = 0.27(3).

[c] Occupation = 0.83(3).

TABLE 6
Atomic Parameters for $DMA_6[H_2W_{12}O_{40}] \cdot \sim 4H_2O$

Atom	x/a	y/b	z/c	B_{iso}
W1	0.2325(2)	1/4	0.3694(3)	2.40(9)[a]
W2	0.4961(2)	1/4	0.6532(3)	2.05(9)[a]
W3	0.3639(1)	0.1562(1)	0.2705(2)	2.63(7)[a]
W4	0.4882(1)	0.1569(1)	0.4036(2)	2.41(6)[a]
W5	0.2399(1)	0.1672(1)	0.5921(2)	2.82(7)[a]
W6	0.3813(1)	0.1690(1)	0.7404(2)	2.27(6)[a]
W7	0.3712(1)	0.0749(1)	0.4926(2)	2.58(7)[a]
O1	0.176(3)	1/4	0.282(5)	4.3(15)
O2	0.569(3)	1/4	0.695(4)	2.8(12)
O3	0.348(2)	0.125(2)	0.150(3)	3.2(8)
O4	0.560(2)	0.128(2)	0.360(3)	3.2(8)
O5	0.192(2)	0.112(2)	0.645(4)	4.5(10)
O6	0.378(2)	0.113(2)	0.840(3)	2.8(8)
O7	0.359(3)	−0.011(2)	0.514(4)	5.8(13)
O13	0.285(2)	0.182(2)	0.319(3)	2.6(8)
O15	0.201(2)	0.182(2)	0.459(3)	2.7(8)
O24	0.500(2)	0.184(2)	0.544(3)	1.9(7)
O26	0.469(2)	0.181(1)	0.746(3)	1.9(6)
O33	0.374(3)	1/4	0.244(4)	3.0(11)
O34	0.451(2)	0.140(2)	0.273(3)	4.0(9)
O37	0.355(2)	0.074(2)	0.342(3)	2.0(7)
O44	0.488(2)	1/4	0.371(3)	1.0(8)
O47	0.457(2)	0.071(2)	0.450(4)	4.2(10)
O55	0.206(4)	1/4	0.647(5)	4.6(16)
O56	0.297(2)	0.172(2)	0.696(3)	3.5(9)
O57	0.295(2)	0.104(2)	0.523(3)	3.1(8)
O66	0.371(2)	1/4	0.822(3)	1.3(8)
O67	0.395(2)	0.104(2)	0.626(3)	2.3(7)
O155	0.290(3)	1/4	0.511(4)	1.6(9)
O266	0.398(3)	1/4	0.636(4)	2.9(11)
O347	0.391(2)	0.176(2)	0.433(3)	3.3(9)
N1	0.704(5)	1/4	0.519(7)	5.6(22)
C11	0.766(7)	1/4	0.437(10)	6.9(32)
C12	0.7074	1/4	0.6431	7.7(32)
N2	0.518(3)	0.047(2)	0.668(4)	3.6(11)
C21	0.586(5)	0.083(4)	0.685(8)	7.7(24)
C22	0.5002	0.0101	0.7575	7.7(24)
N3	0.0283	1/4	0.4449	7.7(24)
C31	0.0438	1/4	0.5225	7.7(24)

[a] $B_{eq} = 1/3[B_{11}a^{*2}a^2 + B_{22}b^{*2}b^2 + B_{33}c^{*2}c^2 + 2B_{12}a^*b^*ab \cdot \cos\gamma + 2B_{13}a^*c^*ac \cdot \cos\beta + 2B_{23}b^*c^*bc \cdot \cos\alpha]$.

resulting atomic coordinates and isotropic (equivalent) temperature parameters are shown in Table 6.

DISCUSSION

As already mentioned in the Introduction and Experimental sections, tungsten trioxide forms various structures depending on the preparation conditions, as well as the cation templates incorporated in the parent framework. The cubic perovskite phase only forms with small cations such as Li^+ and H^+, while the hexagonal and pyrochlore phases can be obtained with larger cations. To investigate the impact of cation templates on WO_3 framework structures, a strategy of using ammonium NH_4^+ as a starting template was pursued. Then the hydrogen in NH_4^+ was gradually replaced one by one with methyl groups (CH_3) to increase the size of the template.

In the case of NH_4^+ and MA cations, both hexagonal and pyrochlore phases were formed depending on the pH of the reaction solution and the heating temperature of the hydrothermal synthesis. Lower pH and higher temperature tend to form the more thermodynamically stable hexagonal phases. Higher pH and lower temperature lead to the formation of the pyrochlore phase. Stoichiometric pyrochlore has the general formula $A_2B_2O_6O'$ with four crystallographically nonequivalent kinds of atoms in the space group $Fm3m$. The framework tungsten and oxygen atoms are located in 16*c* (0, 0, 0) and 48*f* (0.31, 1/8, 1/8), respectively, while the incorporated atoms occupy 16*d* (1/2, 1/2, 1/2), 32*e* (0.43, x, x), and 8*b* (3/8, 3/8, 3/8) sites. The Rietveld refinements of both pyrochlore structures NH_4^+ (A) and MA (B) were carried out. The difference Fourier synthesis and the following refinement of the occupation factors made it possible to find a distribution of the cations. The results are shown in Table 2, and are consistent with earlier reports (8–10). A more complete discussion of the pyrochlore and hexagonal bronze structure investigation can be found elsewhere (11).

Unlike relatively small NH_4^+ and MA cations, use of the larger cations, such as ammonium substituted by two to four methyl groups, does not lead to formation of the "expected" open framework structures. Only in some cases, at higher temperature, the formation of the hexagonal bronze in the form of a slightly crystalline blue powder can be observed (Table 1). We conclude that formation is not determined by large ammonium cations, but by temperature and pH in the same way as in the case of relatively small cations. The regular products of this kind of interaction are well-shaped crystals of C–E compounds, that are different shades of blue, or even colorless. Their IR spectra clearly show the formation of the dodecatungstate cluster. That anion presents the well-known cluster the structure of which has been reported for the first time in 1934 by Keggin (12). Usually, the Keggin cluster $[XW_{12}O_{40}]^{-n}$ holds a heteroatom X such as Si in $TMA_4[SiW_{12}O_{40}]$ (13), P in $(H_5O_2^+)_3[PW_{12}O_{40}^{-3}]$ (14), and many other small cations (15, p. 58), as well as two protons (12, 15–17), or even the Cu^{+2} cation in a statistic couple with two hydrogen atoms (19). The structure with three hydrogen atoms per cluster $[H_3W_{12}O_{40}]^{-5}$ was also reported (18), but this composition was based on charge balance, and not on complete structure determination. NMR studies (15, p. 52, 16) prove that the Keggin anion holds two hydrogen atoms. This fact allows the use of the polyanion cluster formula $[H_2W_{12}O_{40}]^{-6}$ and TGA weight losses to calculate our novel compounds' composition (Table 2).

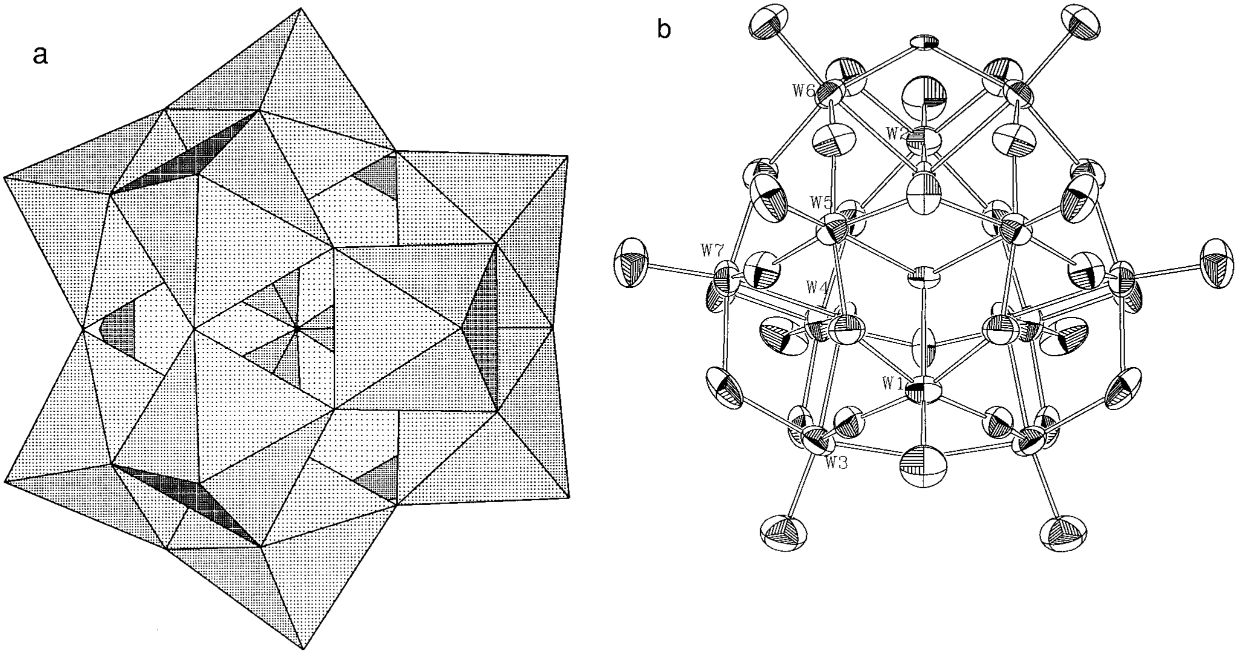

FIG. 3. The Keggin cluster represented by W polyhedra (a) and thermal motion ellipsoids (b) with 50% probability.

The formation of Keggin compounds, when DMA, TrMA, and TMA are used, shows that these large cations no longer play a role as template ions in the interaction with tungsten oxide. They are large enough to provide a positive charge balance to the thermodynamically stable polyanionic tungsten cluster $[H_2W_{12}O_{40}]^{-6}$. In contrast, the TMA cation reacts with molybdenum oxide to form the layered monoclinic bronze, $TMA[Mo_4O_{12}]$, that is described in our previous work (4). Moreover, our attempt to use long chain amines, such as dodecyltrimethylammonium (DTA), $CH_3(CH_2)_{11}N(CH_3)_3^+$, yields the formation of tungsten Keggin clusters in the same ratio 1 dodecatungstate anion per 6 DTA cations (20, 21), while an interaction of the molybdenum oxide with this amine leads again to a layered structure (20, 21).

The quality of the crystals obtained only allowed us to do a full structure determination from single crystal data for only two of the novel compounds, $DMA_6[H_2W_{12}O_{40}] \cdot {\sim}4H_2O$ (*D*) and $TMA_6[H_2W_{12}O_{40}] \cdot 2H_2O$ (*G*). In the case of the *F* compound with TrMA, the space group, cell parameters, composition (Table 2), and powder diffraction patterns (Figs. 2d, 2e) indicate it is isostructural to the *G* compound. The *E* compound, that was formed at lower temperature, has a different, twice smaller unit cell. According to the IR spectra and structures, all those compounds are built as ionic crystals by packing huge tungsten polyanions and substituted ammonium cations in a ratio of 1 : 6.

The dodecatungstate cluster of the title compounds exists in its most common α form, that can be described as a cubo-octahedral framework of tungsten atoms. The oxygen atoms form an almost close packed structure with a tetrahedral cavity inside the cluster, which is usually occupied by a heteroatom. The structure of the cluster is

TABLE 7
Bond Length (Å) Comparison in the Keggin Clusters

Compounds	W–O$_{(a)}$	W–O$_{(b)}$	W–O$_{(c)}$	W–O$_{(d)}$	Ref.
$DMA_6[H_2W_{12}O_{40}] \cdot {\sim}4H_2O$	1.70–1.75(5)	1.88–1.99(5)	1.84–1.97(4)	2.12–2.24(4)	this work
$TMA_6[H_2W_{12}O_{40}] \cdot 2H_2O$	1.68–1.73(3)	1.90–1.92(2)	1.91–1.97(2)	2.15–2.27(2)	this work
$TMA_6[(Cu, H_2)W_{12}O_{40}] \cdot 5H_2O$	1.70(5)	1.88(4)	1.94(4)	2.22(4)	(16)
$TMA_6[H_2W_{12}O_{40}] \cdot 9H_2O$	1.71(4)	1.91(5)	1.96(9)	2.22(9)	(14)
$TMA_4[SiW_{12}O_{40}]$	1.69–1.74(2)	1.88–1.98(2)	1.86–1.95(2)	2.33–2.37(2)	(10)
$Rb_4H_8[H_2W_{12}O_{40}] \cdot {\sim}18H_2O$	1.69(2)	1.97(2)	1.91(2)	2.32(2)	(13)

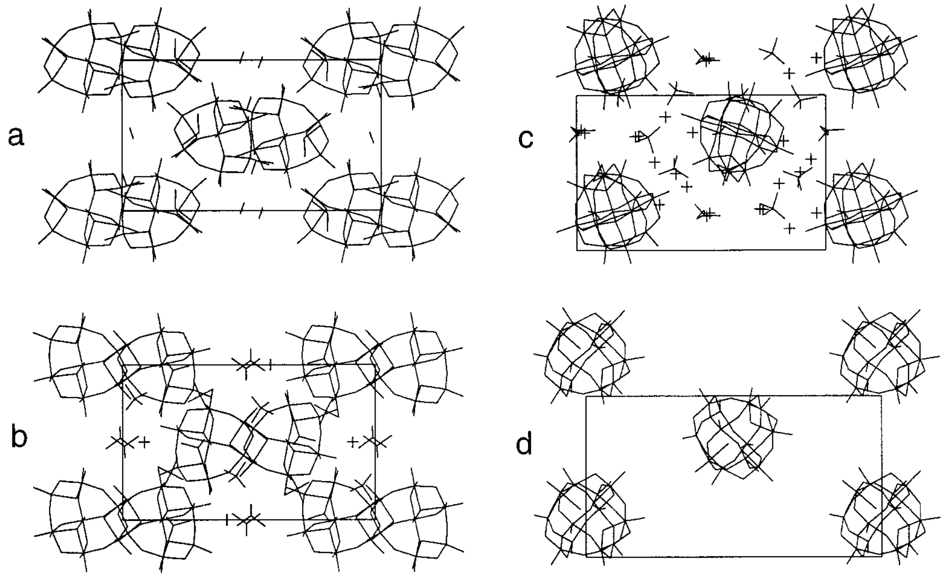

FIG. 4. The close packed layers of the dodecatungstate clusters in (a) $DMA_6[H_2W_{12}O_{40}] \cdot \sim 4H_2O$, (b) $TMA_6[H_2W_{12}O_{40}] \cdot 2H_2O$, (c) $TMA_6[(Cu, H_2)W_{12}O_{40}] \cdot 5H_2O$, and (d) $TrBA_5[H_3W_{12}O_{40}]$.

represented by W polyhedra in Fig. 3b. This cluster can be shown as the usual arrangement of four W_3O_{13} groups, each of them in association with three edge-sharing WO_6 octahedra. Four kinds of oxygen atoms are present. The first O(a) is double bonded with one tungsten atom. The second and third, O(b) and O(c), are neighbored with two tungsten atoms, but O(b) is shared by different W_3O_{13} groups. The last, O(d), is common to three tungsten octahedra in the range of the same W_3O_{13} group. Accordingly, they have different W–O distances that are compared for different Keggin compounds in Table 7. The shortest W–O(a) distances agree with the W–O double bond length.

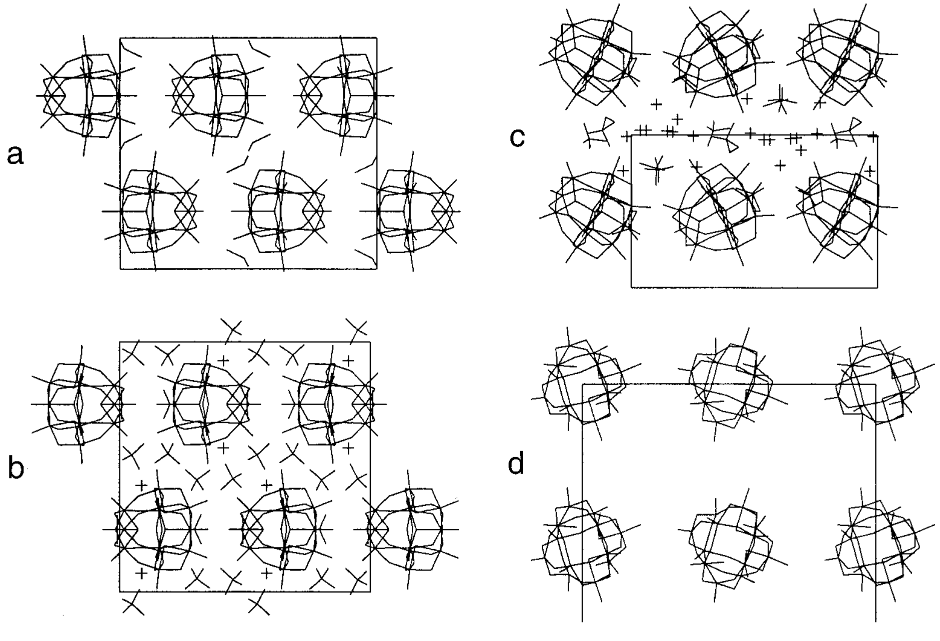

FIG. 5. Different packing of the Keggin cluster layers in (a) $DMA_6[H_2W_{12}O_{40}] \cdot \sim 4H_2O$, (b) $TMA_6[H_2W_{12}O_{40}] \cdot 2H_2O$, (c) $TMA_6[(Cu, H_2)W_{12}O_{40}] \cdot 5H_2O$, and (d) $TrBA_5[H_3W_{12}O_{40}]$.

The O(d) atoms have the longest distances, and form a tetrahedron inside the cluster. This empty tetrahedron is usually occupied in heterotungstates. The three ranges of W–O distances distribution agree with the IR absorption peaks, which are in the accepted range for W–O vibrations.

There are three different compounds in the system TMA–Keggin cluster–water with the same 6:1 ratio TMA/W cluster, but with different content of water–nanohydrate (17), pentahydrate (5), and the title *G* compound–dihydrate. The difference between them is packing of the ions and the connection of anions by H bonds. The much larger and heavier cluster anions play the most important role in the formation of the structure. In all those cases, as well as in the case of the *D* compound with DMA, the Keggin clusters form the close packed layers that are present in Fig. 4. This causes the specific $1:\sqrt{3}$ ratio between the two cell parameters that are parallel to the layer. The stacking of those layers depends on how much of the filling material, such as cations and water, they include. A hexagonal close packing of the cluster layers is clearly seen in Figs. 5a–5c, but in the case of $\mathrm{TrBA_6[H_3W_{12}O_{40}]}$ (18), where a huge tributylammonium cation (TrBA) is present, the layers are packed differently (Fig. 5d). The tungstate cluster of the *G* structure is surrounded by 12 cations in such a way that each of them is placed in front of the square or triangular face of a cubo-octahedron. At the same time, the TMA cations are located around the center of triangles, that are formed by W clusters, but not in the tetrahedral or octahedral cavities.

The crystalline water present yields some additional H bonding of the anionic clusters in the layers. In the case of the *G* compound, the lone water molecule connects the W cluster along the *c* axis by two strong H bonds with the terminal oxygen atoms ($O_4 \cdots O_w = 2.80(3)$, $O_5 \cdots O_w = 2.84(3)$ Å, angle $O_4–O_w–O_5 = 101.9(9)°$). This fact and the absence of distances to oxygen atoms short enough validate the presence of water molecules, but not that of H_3O^+, hydroxonium ions.

Powder reflections listings (hkl, intensities, d_{obs}, d_{clc}) and tables of anisotropic thermal parameters are available.[1]

ACKNOWLEDGMENTS

The work of Binghamton was supported by the National Science Foundation through Grants DMR 8913849 and 9422667. We also thank Professor Suematsu of the Physics Department at the University of Tokyo for hosting one of us (MSW) on a JSPS Fellowship during which part of this work was performed and where the magnetic susceptibility measurements were made. The initial work of Ken Reis on the ammonium tungstates is acknowledged.

REFERENCES

1. K. P. Reis, A. Ramanan, and M. S. Whittingham, *Chem. Mater.* **2,** 219 (1990).
2. J.-D. Guo, K. P. Reis, and M. S. Whittingham, *Solid State Ionics* **53–56,** 305 (1992).
3. J.-D. Guo, P. Zavalij, and M. S. Whittingham, *Eur. J. Solid State Chem.* **31,** 833 (1994).
4. J.-D. Guo, P. Zavalij, and M. S. Whittingham, *Chem. Mater.* **6,** 357 (1994).
5. E. K. Hodorowicz, *Acta Chim. Hung.* **125,** 839 (1988).
6. L. G. Akselrud, P. Zavalij, Yu. N. Grin, V. K. Pecharsky, B. Baumgartner, and E. Wolfel, "2nd European Powder Diffraction Conference: Abstr. of papers," p. 41. Enschede, The Netherlands, 1992; *Mater. Sci. Forum* 133–136 (1993).
7. G. M. Sheldrick, "SHELX 76. Program for crystal structure determination." Univ. Cambridge, England, 1976.
8. R. Nedjar, M. M. Borel, M. Hervieu, and B. Raveau, *Mater. Res. Bull.* **23,** 91 (1988).
9. J. R. Günter, M. Amberg, and H. Schmalle, *Mater. Res. Bull.* **24,** 289 (1989).
10. M. Figlarz, *Chem. Scripta* **28,** 3 (1988).
11. (a) J.-D. Guo, Ph.D. Thesis, SUNY Binghamton, 1994; (b) K. P. Reis, A. Ramanan, and M. S. Whittingham, *J. Solid State Chem.* **96,** 31 (1992).
12. J. F. Keggin, *Proc. R. Soc. London Ser. A.* **144,** 75–100 (1934).
13. J. Fuchs, A. Thiele, and R. Z. Palm, *Naturforsch. B* **36,** 161 (1981).
14. G. M. Brown, M.-R. Noe-Spirlet, W. R. Busing, and H. A. Levy, *Acta Crystallogr. Sect. B* **33,** 1038 (1977).
15. M. T. Pope, "Heteropoly and Isopoly Oxometalates." Springer-Verlag, Berlin, 1984.
16. Y. Jeannin, J. P. Launay, and M. A. Seid Sedjadi, *Inorg. Chem.* **19,** 2933 (1980).
17. M. Asami, H. Ichida, and Y. Sasaki, *Acta Crystallogr. Sect. C* **40,** 35 (1984).
18. J. Fuchs and E.-P. Flindt, *Z. Naturforsch. B* **34,** 412 (1979).
19. H.-J. Lunk, S. Giese, J. Fuchs, and R. Stösser, *Anorg. Allg. Chem.* **619,** 961 (1993).
20. M. S. Whittingham, J. Li, J.-D. Guo, and P. Zavalij, "Soft Chemistry Routes to New Materials" (J. Rouxel, M. Tournoux, and R. Brec, Eds.), Vol. **152–153**; p. 99. Trans Tech Publications, Nantes, France, 1993.
21. M. S. Whittingham, J.-D. Guo, R. Chen, T. Chirayil, G. Janauer, and P. Zavalij, *Solid State Ionics* **75,** 257 (1995).

---

[1] See NAPS document No. 05298 for 08 pages of supplementary materials. Order from ASIS/NAPS, Microfiche Publications, P.O. Box 3513, Grand Central Station, New York, NY 10163. Remit in advance $4.00 for microfiche copy or for photocopy, $7.75 up to 20 pages plus $.30 for each additional page. All orders must be prepaid. Institutions and Organizations may order by purchase order. However, there is a billing and handling charge for this service of $15. Foreign orders add $4.50 for postage and handling, for the first 20 pages, and $1.00 for additional 10 pages of material, $1.50 for postage of any microfiche orders.